Jour. Fac. Sci., Hokkaido Univ., Ser. IV,
vol. 18, nos. 1-2, Feb., 1978, pp. 215-236

STUDY OF THE SYSTEM $CaMgSi_2O_6$-$CaFe^{3+}AlSiO_6$-$CaAl_2SiO_6$-$CaTiAl_2O_6$*: II. THE JOIN $CaMgSi_2O_6$-$CaAl_2SiO_6$-$CaTiAl_2O_6$ AND ITS BEARING ON Ca-Al-RICH INCLUSIONS IN CARBONACEOUS CHONDRITE

by

Kosuke Onuma and Makoto Kimura

(with 5 tables and 7 text-figures)

(Contribution from the Department of Geology and Mineralogy,
Faculty of Science, Hokkaido University, No. 1535)

Abstract

In the join $CaMgSi_2O_6$-$CaAl_2SiO_6$-$CaTiAl_2O_6$, forsterite, anorthite, spinel, perovskite, and clinopyroxene(ss) crystallize as the primary phases. Spinel has the widest liquidus field. Perovskite has a small liquidus field, but it is present at the subliquidus and subsolidus temperatures. Forsterite is consumed by the reaction with liquid at about 1250°C. Melilite does not have its own liquidus field, but crystallizes below the temperature of 1250°–1300°C as a subliquidus and subsolidus phase. Two clinopyroxenes(ss) were found in the join: one is Ti-bearing diopside(ss) and the other is Ti-pyroxene(ss) containing TiO_2 up to 8.7%. The liquidus temperature of Ti-pyroxene(ss) ranges from 1234°C to 1250°C and its liquidus field is bounded by that of forsterite, diopside(ss), perovskite, spinel and anorthite. Four univariant assemblages are encountered: spinel + anorthite + melilite + Ti-pyroxene(ss) + liquid, spinel + anorthite + melilite + perovskite + liquid, anorthite + melilite + perovskite + Ti-pyroxene(ss) + liquid, and spinel + anorthite + melilite + diopside(ss) + liquid. An invariant point spinel + anorthite + melilite + perovskite + Ti-pyroxene(ss) + liquid was confirmed at 1230°C. Two invariant points are assumed from the distribution of univariant lines: diopside(ss) + anorthite + Ti-pyroxene(ss) + perovskite + melilite + liquid, and spinel + anorthite + melilite + Ti-pyroxene(ss) + diopside(ss) + liquid. The chemical composition of the Ti-pyroxene(ss) is very close to that of clinopyroxene found in Ca-Al rich inclusions of the Allende meterorite. This clinopyroxene coexists with spinel, perovskite, melilite, and anorthite and this assemblage is the same as that of the invariant point confirmed in the present study. From the observation mentioned above, the join $CaMgSi_2O_6$-$CaAl_2SiO_6$-$CaTiAl_2O_6$ is related to the formation of the inclusions in the Allende meteorite. The bulk compositions of the Type B inclusions (Grossman, 1975) are calculated in terms of $CaMgSi_2O_6$, $CaAl_2SiO_6$, $CaTiAl_2O_6$, and $MgAl_2O_4$ (spinel), and projected to the join. The possible formation mechanism of the inclusions is discussed with reference of the crystallization of the join.

Introduction

Yagi and Onuma (1969) studied the role of Ti in the alkalic rocks and

* This is one of a series of experimental studies of a fassaitic pyroxene model. Part I is "The join $CaMgSi_2O_6$-$CaAl_2SiO_6$-$CaFeAlSiO_6$ in air and its bearing on fassaitic pyroxene" which appears in Jour. Fac. Sci., Hokkaido Univ. Ser. IV, vol. 16, 343-356, 1975.

found that the clinopyroxene(ss) (ss: solid solution) in the system diopside-akermanite-nepheline-$CaTiAl_2O_6$ contains a considerable amount of TiO_2. Later they showed that clinopyroxenes(ss) in the alkalic rocks are fassitic and consist mainly of $CaMgSi_2O_6$ (Di) $CaAl_2SiO_6$ (CaTs), $CaFe^{3+}AlSiO_6$ (FATs), and $CaTiAl_2O_6$ (Tp) (Onuma and Yagi, 1970, 1975).

Diopside contains 11 wt.% of Tp (4 % TiO_2) in the join Di-Tp. However, it is assumed that diopside becomes able to contain more TiO_2 with the influence of other molecules in the system Di-FATs-CaTs-Tp (Onuma and Yagi, 1975). Recently Ti-Al-rich pyroxene was found in Ca-Al rich inclusions of the Allende meteorite and its TiO_2 content attains as much as 17% (Mason, 1974; Grossman, 1975). The constituent molecules of this Ti-Al-rich pyroxene are Di, CaTs, and Tp (Mason, 1974) and therefore the present join is significant to the discussion on the formation of Ca-Al-rich inclusions in the carbonaceous chondrite.

In the present paper, the data of the join Di-CaTs-Tp are presented and a discussion on the formation of Ca-Al-rich inclusions is given in terms of the crystallization of the compositions in the join Di-CaTs-Tp.

Experimental Results And Discussions

In the present investigation the ordinary quenching method was employed at 1 atm. The starting materials were prepared by complete crystallization of homogeneous glasses at 900°C. The furnaces used in quenching experiments were regulated to a precision of ±1°C for short duration runs and ±5°C for long duration runs. Pt-$Pt_{87}Rh_{13}$ thermocouples used to measure the temperature were calibrated at the standard melting points of Au (1062°C) and diopside (1391.5°C). The results of quenching experiments are given in Table 1.

Table 1 Results of the quenching experiments of the join $CaMgSi_2O_6$-$CaAl_2SiO_6$-$CaTiAl_2O_6$

Composition(wt.%) Di	CaTs	Tp	Temp. (°C)	Time (hr)	Results
80	10	10	1305	44	gl
			1300	24	di + gl
			1200	168	di
70	20	10	1265	20	gl
			1260	30	di + gl
			1220	240	di + (an) + (gl)
			1200	168	di + (mel) + (an)

Table 1 continued

Composition(wt.%) Di	CaTs	Tp	Temp. (°C)	Time (hr)	Results
67	23	10	1255	24	gl
			1250	72	di
			1245	168	di + an + gl
			1230	168	di + an + gl
			1200	336	di + an
65	25	10	1235	18	gl
			1230	20	cpx + gl
			1220	70	cpx + gl
			1215	168	cpx + an + gl
			1210	168	cpx + an + (gl)
			1200	168	cpx + an + mel
60	30	10	1260	24	gl
			1255	20	an + gl
			1250	70	an + sp + gl
			1245	70	an + sp + cpx + gl
			1220	240	an + sp + cpx + gl
			1240	240	an + sp + cpx + mel + gl
58	32	10	1255	20	gl
			1200	70	an + gl
			1240	168	an + cpx + gl
			1230	168	an + cpx + gl
			1220	168	cpx + an + mel + sp
55	35	10	1310	18	gl
			1305	3	sp + gl
			1260	48	sp + gl
			1255	24	sp + an + gl
			1230	168	sp + an + gl
			1225	168	sp + an + cpx + gl
50	40	10	1355	20	gl
			1350	20	sp + gl
			1305	48	sp + gl
			1300	24	sp + an + gl
			1240	168	sp + an + gl
			1235	240	sp + an + cpx + (mel) + gl
			1220	240	sp + an + cpx + (mel) + gl
			1210	240	loose powder
40	50	10	1440	1	gl
			1430	2	sp + gl
			1335	22	sp + an + gl
			1330	22	sp + an + mel + gl
			1230	240	sp + an + mel + gl
			1220	240	sp + an + mel + gl
			1210	240	cpx + sp + an + mel
30	60	10	1460	1	gl
			1450	1	sp + gl
			1355	20	sp + gl
			1350	20	sp + an + gl

Table 1 continued

Composition(wt.%) Di	CaTs	Tp	Temp. (°C)	Time (hr)	Results
30	60	10	1250	48	sp + an + mel + gl
			1245	168	sp + an + mel + gl
			1240	240	sp + an + mel + pv + gl
			1220	240	sp + an + mel + pv + gl
			1210	240	sp + an + mel + pv + gl?
			1200	168	sp + an + mel + pv + cpx
60	27	13	1240	20	gl
			1235	20	Ti-px + an + gl
70	15	15	1255	24	gl
			1250	72	di + gl
65	20	15	1240	20	gl
			1235	20	Ti-px + gl
73	10	17	1265	48	gl
			1260	72	di + fo + gl
			1255	20	di + gl
			1225	168	di + gl
			1220	168	di + pv + gl
72	9	19	1250	72	gl
			1245	20	fo + gl
			1240	24	di + gl
			1225	168	di + gl
			1220	168	di + pv + (gl)
			1200	168	di + pv
62	20	18	1240	168	gl
			1235	168	sp + gl
			1230	240	sp + gl
			1225	240	sp + Ti-px + gl
			1220	288	Ti-px + an + pv + gl
70	10	20	1265	20	gl
			1260	20	fo + gl
			1255	48	fo + di + gl
			1250	48	di + gl
			1235	240	di + gl
			1230	240	di + pv + gl
			1200	168	di + pv
68	12	20	1240	24	gl
			1235	20	fo + gl
			1230	168	di + gl
			1225	168	di + gl
			1220	168	di + pv + gl
			1200	168	cpx + pv
65	15	20	1250	48	gl
			1245	72	Ti-px + gl
			1225	168	Ti-px + gl
			1220	168	cpx + pv + gl
			1200	168	cpx + pv

Table 1 continued

Composition(wt.%) Di	CaTs	Tp	Temp. (°C)	Time (hr)	Results
60	20	20	1275	72	gl
			1270	24	sp + gl
			1245	168	sp + gl
			1240	240	sp + Ti-px + an + gl
			1235	168	Ti-px + an + gl
			1200	240	Ti-px + an + pv + mel
50	30	20	1390	2	gl
			1380	3	sp + gl
			1285	72	sp + gl
			1280	46	sp + an + gl
			1270	46	sp + an + gl
			1260	48	sp + an + mel + gl
			1245	168	sp + an + mel + gl
			1240	192	sp + an + mel + Ti-px + gl
			1235	168	sp + an + mel + Ti-px + gl
			1230	168	sp + an + mel + Ti-px + pv + (gl)
			1200	168	sp + an + mel + Ti-px + pv
40	40	20	1445	1	gl
			1440	1	sp + gl
			1310	23	sp + gl
			1305	48	sp + an + gl
			1265	72	sp + an + gl
			1260	48	sp + an + pv + gl
			1250	45	sp + an + pv + mel + gl
			1235	240	sp + an + pv + mel + gl
			1230	240	sp + an + pv + mel + Ti-px + gl
			1200	240	sp + an + pv + mel + Ti-px
30	50	20	1450	2	gl
			1445	1	sp + gl
			1335	22	sp + gl
			1330	22	sp + an + gl
			1320	18	sp + an + mel + gl
			1295	20	sp + an + mel + gl
			1290	20	sp + an + mel + pv + gl
			1230	168	sp + an + mel + pv + gl
			1225	240	sp + an + mel + pv + Ti-px
69	10	21	1260	70	gl
			1255	18	fo + di + gl
			1250	20	fo + di + gl
			1245	70	di + gl
			1235	168	cpx + pv + gl
			1230	168	cpx + pv + gl
			1200	168	cpx + pv
69	8	23	1260	24	gl
			1255	20	fo + di + gl
			1260	24	gl
			1255	20	fo + di + gl
			1250	168	di + gl

Table 1 continued

Compositions(wt.%) Di	CaTs	Tp	Temp. (°C)	Time (hr)	Results
69	8	23	1245	168	di + gl
			1240	168	di + pv + gl
			1200	168	cpx + pv
67	10	23	1250	48	gl
			1245	72	Ti-px + gl + pv
			1200	168	Ti-px + pv
65	10	25	1265	20	gl
			1260	20	sp + gl
			1225	18	sp + gl
			1220	72	sp + Ti-px + gl
			1210	168	Ti-px + pv + gl
67	3	30	1250	48	gl
			1245	168	Ti-px + pv + gl
			1200	168	Ti-px + pv
65	5	30	1240	20	gl
			1235	70	Ti-px + gl
			1230	70	Ti-px + pv + gl
			1210	168	Ti-px + pv + (gl)
			1200	168	Ti-px + pv
60	10	30	1320	8	gl
			1310	20	sp + gl
			1245	168	sp + gl
			1240	168	sp + Ti-px + pv + gl
			1200	168	sp + Ti-px + pv
50	20	30	1405	1	gl
			1400	1	sp + gl
			1265	72	sp + gl
			1260	48	sp + pv + an + gl
			1240	168	sp + pv + an + gl
			1235	240	sp + pv + an + Ti-px + gl
40	30	30	1460	1	gl
			1450	1	sp + gl
			1280	168	sp + pv + an + mel + gl
			1230	168	sp + pv + an + mel + Ti-px + gl
			1225	240	sp + pv + an + mel + Ti-px
30	40	30	1470	1	sp + gl
			1310	20	sp + gl
			1305	48	sp + an + pv + gl
			1300	168	sp + an + pv + mel + gl
			1230	168	sp + an + pv + mel + gl
			1225	240	sp + an + pv + mel + Ti-px
66	1	33	1245	72	gl
			1240	24	pv + cpx + gl
50	10	40	1430	1	gl
			1420	1	sp + gl
			1310	20	sp + gl

Table 1 continued

Compositions(wt.%) Di	CaTs	Tp	Temp. (°C)	Time (hr)	Results
50	10	40	1305	48	sp + pv + gl
			1280	46	sp + pv + mel + gl
			1265	72	sp + pv + mel + gl
			1260	48	sp + pv + an + mel + gl
			1235	240	sp + pv + an + mel + gl
			1230	264	sp + pv + an + mel + Ti-px + gl
40	20	40	1470	1	sp + gl
			1340	18	sp + gl
			1335	22	sp + pv + gl
			1305	44	sp + pv + gl
			1300	46	sp + pv + an + gl
			1250	96	sp + pv + an + mel + gl
			1235	240	sp + pv + an + mel + gl
			1230	264	sp + pv + an + mel + Ti-px
30	30	40	1470	1	sp + gl
			1355	16	sp + gl
			1350	46	sp + pv + gl
			1305	24	sp + pv + gl
			1300	46	sp + pv + au + gl
			1250	96	sp + pv + an + mel + gl
			1200	168	sp + pv + an + mel + Ti-px
40	10	50	1370	18	sp + gl
			1360	18	sp + pv + gl
			1305	70	sp + pv + gl
			1300	46	sp + pv + an + gl
			1250	96	sp + pv + an + mel + gl
			1200	336	sp + pv + an + mel + Ti-px
30	20	50	1315	72	sp + gl
			1310	20	sp + an + pv + gl
			1300	46	sp + pv + an + mel + gl

di, diopside; an, anorthite; mel, melilite; sp, spinel; pv, perovskite; Ti-px, Ti-pyroxene; cpx, diopside and/or Ti-pyroxene; gl, glass

Liquidus diagram

Fig. 1 shows the liquidus diagram of the join Di-CaTs-Tp. Spinel, perovskite, forsterite, and anorthite appear as the primary phases and it is noticed that the primary field of clinopyroxene(ss) is divided into two fields by the forsterite field as shown in Fig. 1. This fact indicates that the two types of clinopyroxenes(ss) crystallize as the primary phase. One is diopside(ss) and the other is Ti-rich pyroxene(ss) containing more than 7% TiO_2. The primary field of Ti-pyroxene(ss) is bounded by those of spinel, perovskite, forsterite, diopside(ss), and anorthite.

The join Di-CaTs-Tp is a part of the quinary system CaO-MgO-Al_2O_3-TiO_2-SiO_2, so that the points A, B, C, D, and E in Fig. 1 where three crystlline phases coexist with liquid are neither piercing points nor invariant points. The temperature of these points show the beginning of the divariant assemblage in the join. The temperatures, compositions, and phase assemblage of these points are as follows:

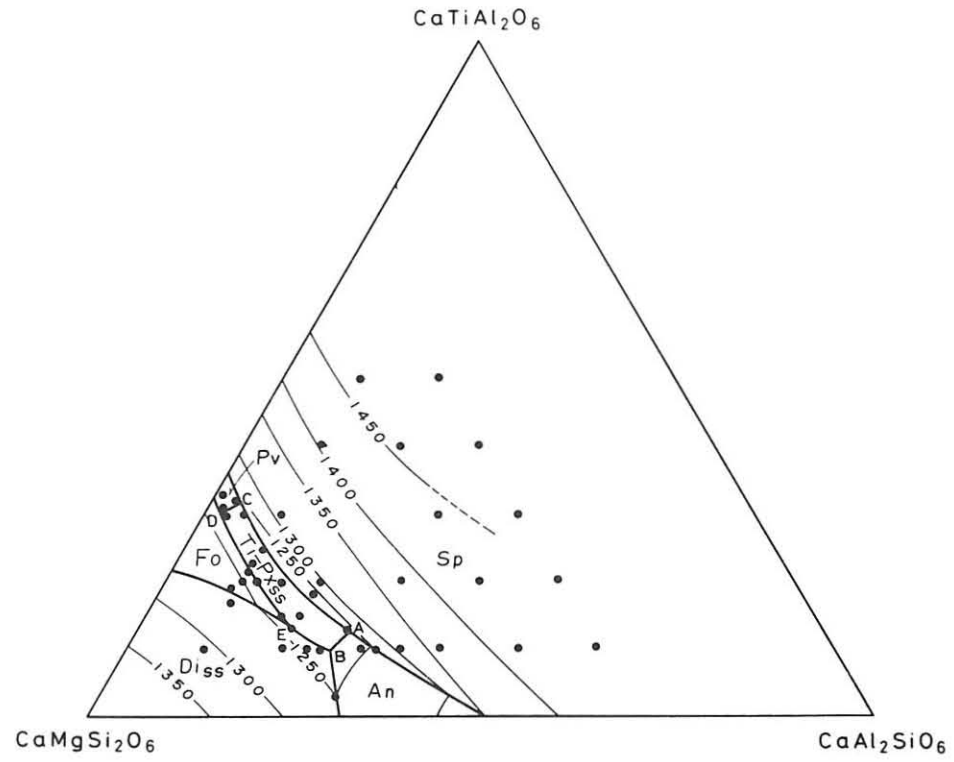

Fig. 1 Liquidus diagram of the join $CaMgSi_2O_6$-$CaAl_2SiO_6$-$CaTiAl_2O_6$. Di_{ss}=diopside$_{ss}$, Fo=forsterite, An=anorthite, Ti-Px_{ss}=Ti-pyroxene$_{ss}$, Pv=perovskite, Sp=spinel

A = spinel + Ti-pyroxene(ss) + anorthite + liquid,
1235°C, [Di(60)CaTs(27)Tp(13)]
B = diopside(ss) + Ti-pyroxene(ss) + anorthite + liquid,
1324°C, [Di(64)CaTs(26)Tp(10)]
C = spinel + perovskite + Ti-pyroxene(ss) + liquid,
1260°C, [Di(65)CaTs(3)Tp(32)]
D = forsterite + perovskite + Ti-pyroxene(ss) + liquid,
1235°C, [Di(68)CaTs(2)Tp(30)]
E = diopside(ss) + Ti-pyroxene(ss) + forsterite + liquid,
1240°C [Di(68)CaTs(17)Tp(15)]

Phase relation in the subliquidus and subsolidus region

Figs. 2 and 3 show the Di(80)Tp(20)-CaTs(80)Tp(20) and Di(90)CaTs(10)-Tp(90)CaTs(10) sections, respectively. Forsterite is present as a primary phase

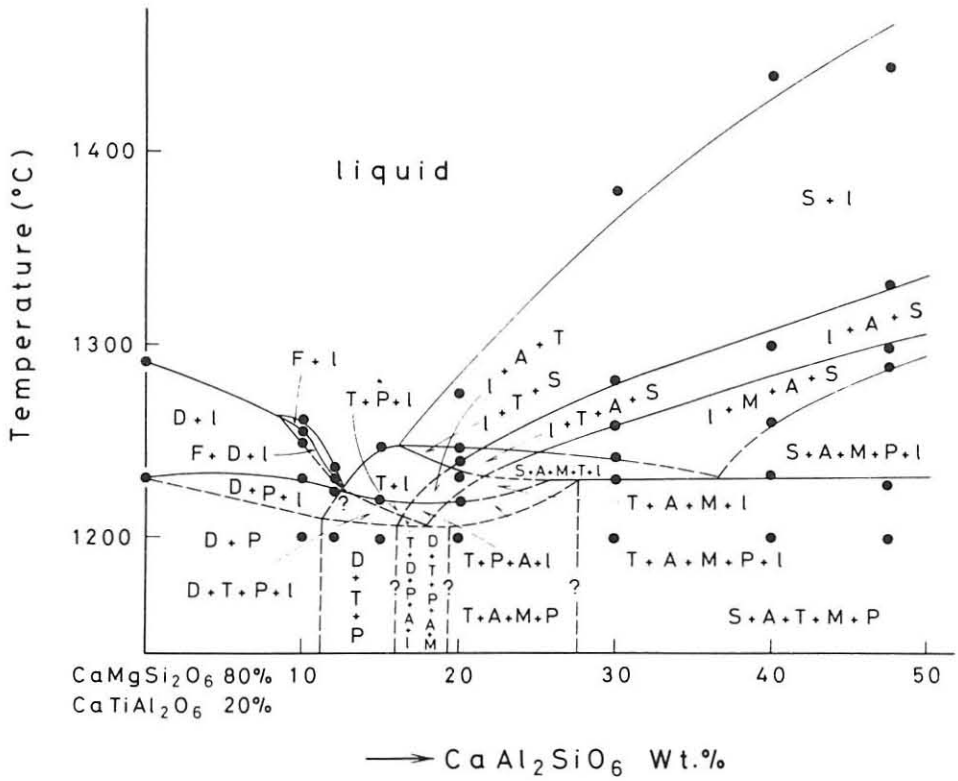

Fig. 2 Phase diagram of the 20 wt% $CaTiAl_2O_6$ section in the join Di-CaTs-Tp. D=diopside$_{ss}$, T=Ti-pyroxene$_{ss}$, F=forsterite, A=anorthite, M=melilite, S=spinel, P=perovskite, l=liquid

but consumed within a narrow temperature range by the reaction with liquid and does not appear in the subsolidus region. Perovskite has very small primary field, but crystallizes in the area rich in Tp (more than 10%) at the subliquidus and subsolidus temperatures. In the composition around Di(60)CaTs(20)-Tp(20) it was observed that spinel disappears at 1235°C, but in the compositions richer in CaTs and Tp the spinel is present both in the subliquidus and subsolidus region. Although melilite does not appear at the liquidus temperatures, it crystallizes at temperatures below 1300°C.

Spinel has a wide crystallization range from the liquidus temperature 1260°C–1500°C to the solidus temperature at about 1210°–1230°C. In the CaTs- and Tp-rich regions it is followed by perovskite, anorthite, or melilite, depending on the starting composition, and finally Ti-pyroxene(ss) joins the assemblage. On the other hand, the crystallization of the composition near the Ti-pyroxene(ss) liquidus field proceeds within a small temperature range 1250°–1210°C. Diopside(ss) appears in the field where Di exceeds about 70%,

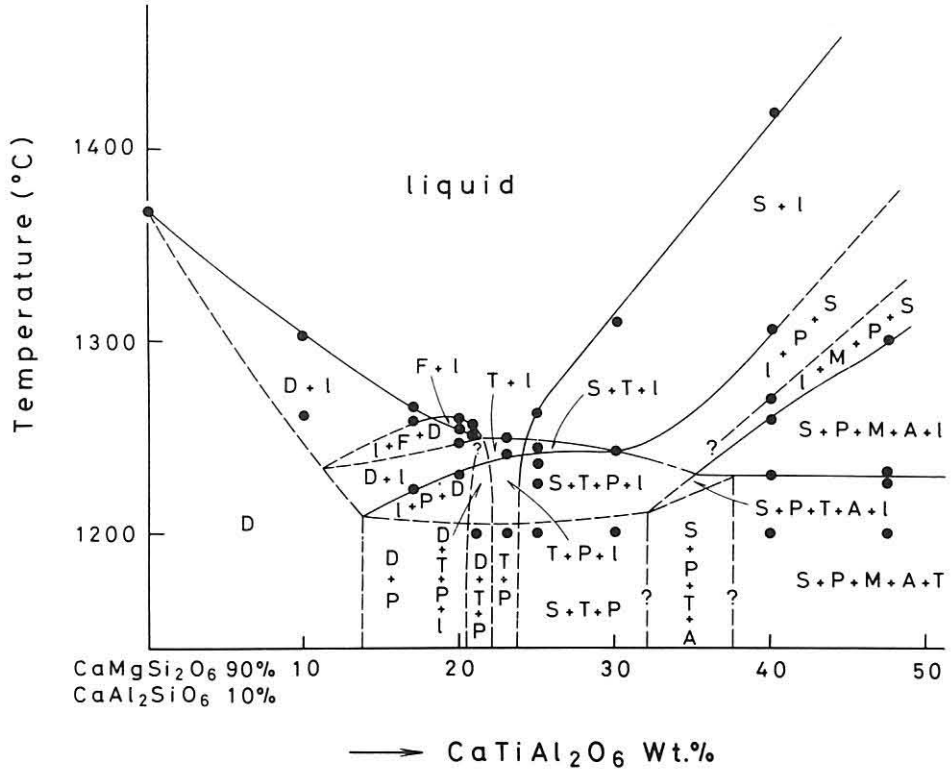

Fig. 3 Phase diagram of the 10 wt% $CaAl_2SiO_6$, in the join Di-CaTs-Tp. Abbreviations are the same as in Fig. 2.

whereas Ti-pyroxene(ss) is present where Di is less than 60%. Between the compositions of 70% Di and 60% Di, judging from the phase relation at the liquidus, there should be a region where the two pyroxenes are coexisting. However, it is difficult to distinguish these two phases as will be mentioned later. Therefore, the parts in Figs. 2 and 3 where the two pyroxenes coexist are constructed by the estimation of the phase relations in the subliquidus regions.

The diopside(ss) single phase field at subsolidus temperatures is observed in the area of composition Di(89)Tp(11)-Di(70)CaTs(15)Tp(15)-Di(85)CaTs(15).

Suggested Flow Sheet

The join Di-CaTs-Tp is a part of the quinary system, so that a six-phase assemblage Ti-pyroxene(ss) + anorthite + spinel + perovskite + melilite + liquid encountered at 1230° C is an isobaric invariant assemblage. Five univariant lines are distributed around the invariant point in the quinary system. In the present study, among the five univariant assemblages, three assemblages were encountered; spinel + melilite + anorthite + perovskite + liquid, anorthite +

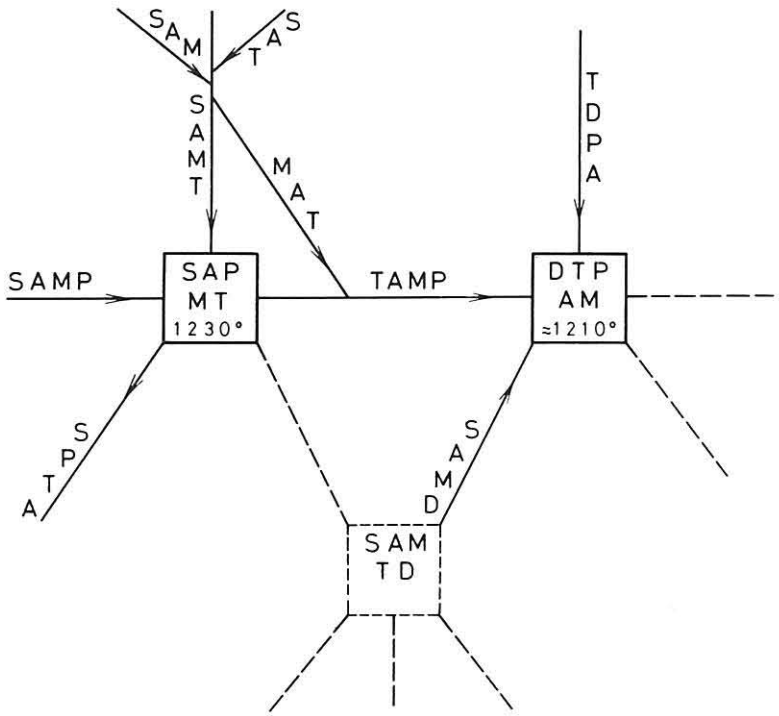

Fig. 4 Relationship between invariant points and univariant lines. Abbreviations are the same as in Fig. 2.

melilite + Ti-pyroxene(ss) + spinel + liquid, and anorthite + melilite + perovskite + Ti-pyroxene(ss) + liquid. The first two univariant assemblages meet at 1230°C, forming an invariant assemblage. From the observation of the disappearence of spinel around 1235°C in some compositions, it is assumed that the invariant point is a reaction point and the spinel is consumed at this point to form the third univariant assemblage excluding spinel. This univariant line attains another invariant point diopside(ss) + Ti-pyroxene(ss) + perovskite + anorthite + melilite + liquid. Unfortunately this assemblage was not confirmed, but it can be assumed from the other data as shown in Fig. 2. The temperature of this invariant point lies at about 1210°C.

Using observations and the estimations mentioned above, a scheme for the relation between the invariant points and the univariant lines is constructed as shown in Fig. 4.

The divariant assemblages spinel + anorthite + melilite + liquid, spinel + anorthite + Ti-pyroxene(ss) + liquid, and anorthite + melilite + Ti-pyroxene(ss) + liquid were found around the univariant assemblage spinel + anorthite + melilite + Ti-pyroxene(ss) + liquid. Spinel is consumed on this univariant line to form the divariant assemblage anorthite + melilite + Ti-pyroxene(ss) + liquid depending on the composition, and the crystallization leaves this univariant line to reach another univariant line anorthite + melilite + Ti-pyroxene(ss) + liquid with falling temperature.

In the 10% Tp section the clinopyroxene seems to be diopside(ss) and the compositions between CaTs(30) and CaTs(50) crystallize into the assemblage diopside(ss) + anorthite + spinel + melilite + liquid. This univariant line probably connects the invariant points diopside(ss) + Ti-pyroxene(ss) + anorthite + perovskite + melilite + liquid and spinel + anorthite + melilite + Ti-pyroxene(ss) + diopside(ss) + liquid as shown in Fig. 4.

Crystalline phases

Clinopyroxene(ss): Diopside(ss) and Ti-pyroxene(ss) form prismatic crystals near the liquidus but forms rounded grains in the subsolidus region. Both phases show similar crystal habit, extinction angle, and color, so that it is very difficult to distinguish these two crystals from each other under the microscope. However, Ti-pyroxene(ss) has higher refractive indices (α = 1.715 and γ = 1.730) than diopside(ss) (α = 1.670–1.685 and γ = 1.700–1.720), and so these two phases are distinguishable by careful examination. However, it was sometimes, very difficult to identify. In that case it is described as clinopyroxene(cpx) in Table 1.

The composition of Di(70)CaTs(15)Tp(15) crystallizes into the diopside(ss) without any other phases. This means the diopside(ss) contains, at least, up to

Table 2 Compositions of Ti-pyroxenes of Type B inclusions (Grossman, 1975) and of the join Di-CaTs-Tp

	DCT System				Type B inclusion					
	$D_{67}C_{10}T_{23}$	$D_{69}C_8T_{23}$	$D_{68}C_{12}T_{20}$	$D_{60}C_{27}T_{13}$	TS8F3-3C	TS23F1-5B	TS12F3-20	TS4F1-4C	TS4F1-1C	TS12F3-21
SiO_2	40.31	39.39	39.50	40.24	41.41	41.97	39.60	39.31	37.08	37.17
TiO_2	7.58	8.71	7.48	4.71	4.28	5.01	6.08	7.02	8.07	9.35
Al_2O_3	14.67	14.44	14.24	16.21	18.38	18.21	18.16	18.20	19.58	19.46
MgO	12.71	11.44	12.24	10.34	10.35	10.52	9.44	9.90	8.62	8.07
CaO	24.80	26.69	25.90	28.53	25.72	25.93	24.94	25.03	25.38	24.77
FeO	–	–	–	–	0.13	<0.03	<0.03	0.49	<0.03	<0.03
Total	100.07	100.67	99.36	100.03	100.27	101.64	98.22	99.95	98.73	98.82
Si	1.46	1.46	1.47	1.51	1.51	1.51	1.47	1.44	1.38	1.38
Al	0.54	0.54	0.53	0.49	0.49	0.49	0.53	0.56	0.62	0.62
Total	2.00	2.00	2.00	2.00	2.00	2.00	2.00	2.00	2.00	2.00
Al	0.11	0.09	0.09	0.20	0.30	0.28	0.27	0.23	0.24	0.23
Ti	0.21	0.24	0.21	0.13	0.12	0.14	0.17	0.19	0.23	0.26
Mg	0.71	0.63	0.68	0.61	0.56	0.56	0.52	0.54	0.48	0.45
Fe	–	–	–	–	0.00	0.00	0.00	0.02	0.00	0.00
Ca	0.98	1.04	1.03	1.08	1.00	1.00	0.99	0.99	1.01	0.99
Total	2.01	2.00	2.01	2.02	1.98	1.98	1.95	1.97	1.96	1.93

D=$CaMgSi_2O_6$, C=$CaAl_2SiO_6$, T=$CaTiAl_2O_6$

15% Tp(5% TiO_2 and 7% Al_2O_3). Yagi and Onuma (1967) showed that diopside incorporates TiO_2 as much as 11% Tp (3.4% TiO_2) in the join Di-Tp. Therefore, it can be said that Tp content in diopside(ss) increases with increasing CaTs in the join Di-CaTs-Tp.

The chemical analyses of Ti-pyroxene(ss) by EPMA are given in Table 2. It is remarkable that the Ti-pyroxene(ss) contains 8% TiO_2 and 14% Al_2O_3. Yang (1973) also synthesized an Ti-rich pyroxene in the same join, which contains 8 – 13% TiO_2. Clinopyroxene containing as much TiO_2 and Al_2O_3 has never been found in terrestrial rocks, but has been found in Ca-Al-rich inclusions of the carbonaceous chondrite (the Allende meterorite). The significance of the present join for these inclusions will be discussed in the later part.

The unit-cell dimensions of diopside(ss) and Ti-pyroxene(ss) are given in Table 3. Both unit-cell volume and c-dimension increase with the increase of Tp content in the join Di-Tp (Onuma et al., 1969). On the other hand, cell volume decreases and c-dimension increases with the increase of CaTs content (Clark et al., 1962). In Fig. 5 the unit-cell volumes are plotted against the c-dimensions.

Table 3 Unit-cell dimensions of the clinopyroxene in the join Di-CaTs-Tp

Comp. of Mix.	a(Å)	b(Å)	c(Å)	β(°)	V(Å³)
$Di_{80}CaTs_{10}Tp_{10}$	9.734(3)	8.867(1)	5.282(2)	106.1(1)	438.0(2)
$Di_{70}CaTs_{20}Tp_{10}$	9.724(7)	8.847(2)	5.288(4)	106.2(1)	436.9(4)
$Di_{60}CaTs_{30}Tp_{10}$	9.711(5)	8.824(3)	5.300(2)	106.0(1)	436.6(3)
$Di_{70}CaTs_{10}Tp_{20}$	9.736(4)	8.858(2)	5.302(2)	106.1(1)	439.0(4)
$Di_{60}CaTs_{20}Tp_{20}$	9.733(7)	8.832(2)	5.308(5)	106.1(1)	438.3(4)
$Di_{50}CaTs_{30}Tp_{20}$	9.734(2)	8.817(1)	5.319(2)	106.2(3)	438.4(2)
$Di_{60}CaTs_{10}Tp_{30}$	9.747(10)	8.834(9)	5.317(7)	105.8(2)	440.5(9)
$Di_{50}CaTs_{20}Tp_{30}$	9.739(3)	8.814(3)	5.324(3)	106.1(4)	439.1(2)
$Di_{65}CaTs_{15}Tp_{20}$	9.745(6)	8.850(3)	5.308(4)	106.0(1)	440.0(4)
$Di_{67}CaTs_{10}Tp_{23}$	9.759(9)	8.847(2)	5.314(5)	105.9(1)	441.4(5)

The line Mg·2Si = Ti·2Al shows the replacement of Tp for Di in the join Di-Tp and the line Mg·Si = Al·Al shows that of CaTs in the join Di-CaTs. The direction of increase of these molecules is shown by the arrows. The clinopyroxene(ss) containing Tp and CaTs should be plotted within the area bounded by the two solid lines. The plots of the present diopside(ss) and Ti-pyroxene(ss) clearly indicate that these clinopyroxenes(ss) contain considerable amounts of TiO_2 and Al_2O_3. The Ti-pyroxene(ss) falls in the area rich in TiO_2 (area B in Fig. 5).

The broken line shows the trend of diopside(ss) crystallized along the join of 10% Tp, indicating that diopside is gradually substituted by CaTs and Tp,

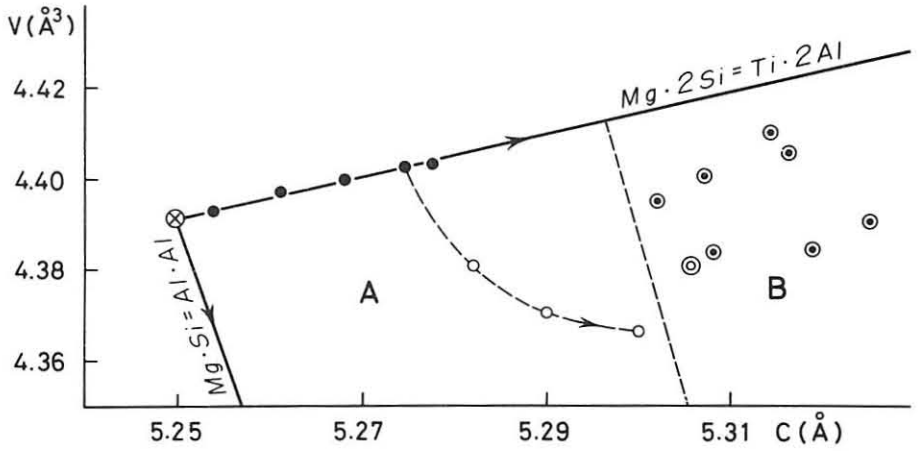

Fig. 5 Variation of uni-cell volume against *c*-dimension. A=area of diopside$_{ss}$, B=area of Ti-pyroxene$_{ss}$

and that Tp in diopside(ss) increases with increasing CaTs.

Other phases: Forsterite usually occurs in colourless stout prismatic crystals, showing high retardation. The refractive indices of forsterite are α = 1.636 and γ = 1.673, indicating that this mineral is pure in composition.

Since melilite occurs at lower temperatures together with other crystals, sometimes it was difficult to identify this mineral under the microscope. The strongest peak of melilite obtained in the present study in X-ray diffraction has values between 31.1° and 31.3° in 2θ, suggesting that the melilite is a solid solution of akermanite and gehlenite.

Anorthite occurs as platy crystals having low birefringence and its 204 reflection is 27.92 in 2θ, indicating that this mineral has pure composition.

Spinel forms small octahedral crystals. Perovskite occurs mainly in minute octahedral or irregular crystals, slightly brownish in color. These two phases are regarded as having essentially definite compositions, as their X-ray diffraction reflections are constant in all of the compositions studied.

Possible Reactions at Subsolidus Temperatures

The phase assemblages at subsolidus temperatures must be derived by the reactions between Di, CaTs, and Tp. The following reactions are assumed for the encountered and suggested subsolidus assemblages.

(1) For the assemblage diopside(ss) and/or Ti-pyroxene(ss) + perovskite:
Di + Tp + CaTs = Pv + 2CaTs + En (En, $MgSiO_3$)

(2) For the assemblage Ti-pyroxene(ss) + anorthite + spinel + perovskite:
2Di + CaTs + 3Tp = 3Pv + 2CaTs + En + Sp + An

(3) For the assemblage diopside(ss) and/or Ti-pyroxene(ss) + anorthite + melilite + perovskite:

$$4Di + 2CaTs + Tp = Pv + 3En + 2An + \underset{\text{melilite}}{Ak} + Geh$$

(4) For the assemblage Ti-pyroxene(ss) + anorthite + melilite + spinel + perovskite:

$$5Di + 2CaTs + 3Tp = 3Pv + Sp + 3An + \underset{\text{melilite}}{Ak} + Geh + 3En$$

(Ak, $Ca_2MgSi_2O_7$; Geh, $Ca_2Al_2SiO_7$)

It is noticed from the reactions mentioned above that clinopyroxene(ss) is expected to contain En and melilite should be a solid solution between Ak and Geh. The Ti-pyroxene(ss) from Di(67)CaTs(10)Tp(23) in Table 2 has En molecules, when calculated in terms of Di, CaTs, and Tp. Sometimes En probably reacts with Tp to produce Pv and MgTs($MgAl_2SiO_6$);

$$MgSiO_3 + CaTiAl_2O_6 = MgAl_2SiO_6 + CaTiO_3$$

Implication Of Ca-Al-rich Inclusion In The Carbonaceous Chondrite

Petrography of Type B Inclusion in the Carbonaceous Chondrite

The mineral assemblage of coarse-grained Ca-Al-rich inclusions in the Allende meterorite (C-3 type meterorite) is close to that of the phase assemblages at subsolidus confirmed in the present study: anorthite + spinel + melilite + Ti-pyroxene(ss) and spinel + perovskite + anorthite + melilite + Ti-pyroxene(ss). Grossman (1975) classified the coarse-grained inclusions into two types; type A consisting mainly of spinel, melilite, and perovskite and type B consisting mainly of Ti-pyroxene, spinel, anorthite, melilite, and rarely perovskite. The chemical compositions of clinopyroxenes are given in Table 3 in comparison with the Ti-pyroxene obtained in the join Di-CaTs-Tp. It is noticed that the chemical compositions of clinopyroxenes in Type B inclusions are similar to those of Ti-pyroxenes obtained in the present study. Spinel is included in melilite, clinopyroxene, and anorthite and is almost pure in composition ($MgAl_2O_4$). Melilite has an average composition $Ak_{25}Geh_{75}$ and sometimes replaces anorthite and clinopyroxene. Anorthite penetrating or surrounding clinopyroxene has the composition An_{99}-An_{100}. Perovskite having almost pure composition ($CaTiO_3$) is included in melilite. Marvin et al. (1970) also reported Ca-Al-rich and Si-poor inclusions consisting of spinel and glass and it seems that this inclusion belongs to Type B inclusions. Blander and Fuchs (1975) also described Ca-Al-rich inclusions. In their 6/1 inclusion spinel and melilite are surrounded by clinopyroxene and an eutectic intergrowth is observed between melilite and clinopyroxene or anorthite and clinopyroxene. Their 10/2 inclusion has gabbroic texture and spinel is included in clinopyroxene, melilite, and anorthite. These two inclusions probably belong to

Type B. Kurat et al. (1975) described Ca-Al-rich inclusions of the Bali meteorite which consists mainly of melilite and clinopyroxene with interstitial anorthite. Spinel is included in almost all of these minerals. The mineral assemblage indicates that this inclusion belongs to Type B.

The petrography mentioned above suggests the following crystallization sequence: Spinel is the earliest phase in crystallization and followed by melilite, anorthite, and Ti-pyroxene which crystallize within a narrow temperature range. Judging from the texture the minerals precipitate from liquid. Blander and Fuchs (1975) suggest that at first Type B inclusions were formed as liquid condensed from the nebula and the constituent minerals crystallized from the liquid with the falling temperature. On the other hand, some workers (Grossman, 1975; Grossman and Clark, 1973; Clayton et al. 1977) claimed that the inclusions were formed as solid by the condensation of gas and then melted to liquid. The two hypotheses indicate, either way, that the inclusion once passed a liquid stage. Therefore, it is reliable to apply the crystallization of some composition in the join Di-CaTs-Tp to the formation of Ca-Al-rich inclusions in the carbonaceous chondrites.

Chemistry and Crystallization of the Composition of Type B Inclusion

The calculated bulk chemical composition of Type B inclusions in the Allende meterorite (Grossman, 1975) are given in Table 4. When the bulk

Table 4 Calculated compositions of Type B inclusions (Grossman, 1975) and Norms

	Chemical composition			
	iii	iv	v	vi
CaO	17.69	18.09	21.45	20.75
Al_2O_3	40.27	37.30	32.81	31.72
TiO_2	2.99	3.68	3.73	4.39
MgO	15.37	14.55	12.03	12.59
SiO_2	23.68	26.36	30.01	30.55
Total	100.00	99.98	100.03	100.00
	Norm			
Di	31.0 (44.8)	31.8 (44.8)	37.7 (44.9)	37.5 (46.0)
Tp	8.8 (12.7)	10.9 (15.3)	11.2 (13.3)	13.1 (16.0)
CaTs	29.4 (42.5)	28.4 (39.9)	35.1 (41.8)	31.0 (38.0)
Sp	31.7	27.0	16.2	16.2
Total	100.9	98.1	100.2	97.8

The figures in parentheses show the projected composition in the join Di-CaTs-Tp
Di=$CaMgSi_2O_6$, Tp=$CaTiAl_2O_6$, CaTs=$CaAl_2SiO_6$, Sp=$MgAl_2O_4$

compositions are calculated in terms of Di, CaTs, Tp, and Sp (spinel $MgAl_2O_4$) the sums of the values make almost 100%, indicating that Type B inclusions belong to the composition tetrahedron Di-CaTs-Tp-Sp in the quinary system CaO-MgO-Al_2O_3-TiO_2-SiO_2. Fig. 6 shows plots of Type B inclusions in the

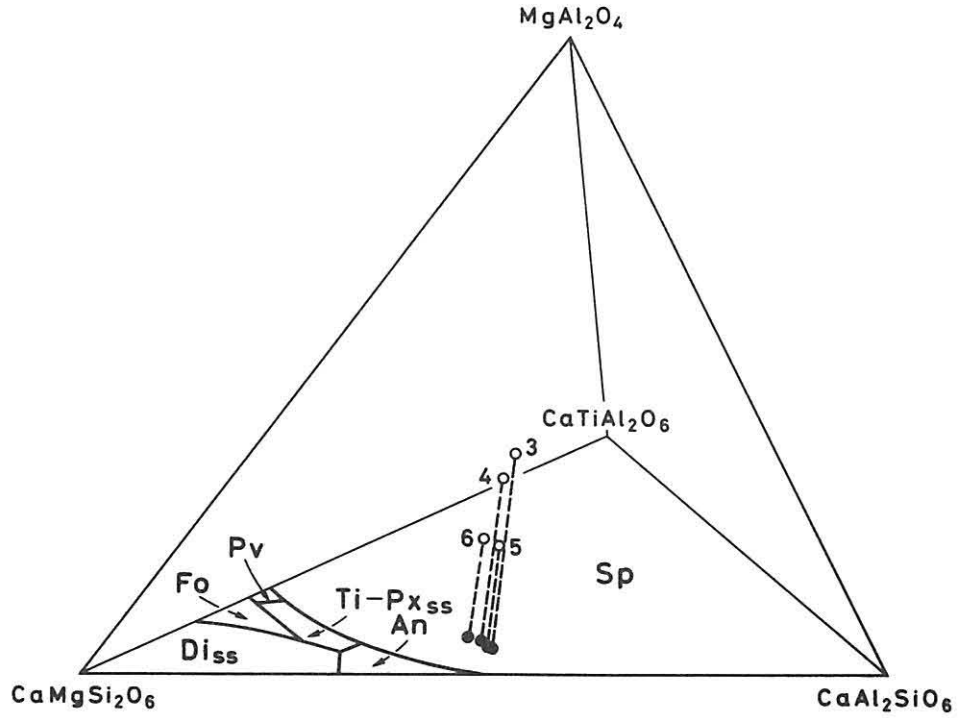

Fig. 6 Plotts of Type B inclusions in the Allende meteorite in the Di-CaTs-Tp-Sp tetrahedron.

tetrahedron. The petrography of the inclusions indicate that spinel is the first phase to appear. The primary field of spinel in the tetrahedron extends from the join Di-CaTs-Tp towards the spinel apex. The plots of the compositions of Type B inclusions fall in the spinel field and with falling temperature liquid reaches the spinel liquidus. With further precipitation of spinel, the liquid moves towards the Di-CaTs-Tp base along the straight line drawn from the spinel apex to the base and reaches the base at points at which bulk compositions of inclusions are projected from the spinel apex to the join Di-CaTs-Tp. After that we can trace the crystallization by the data of the join Di-CaTs-Tp. It is noticed that the projections fall in a narrow area between Di(40)CaTs(40)Tp(20) and Di(50)CaTs(40)Tp(10) as shown in Fig. 7, although the composition of normative spinel ranges from 16% to 32%. The compositions of Type B inclusions begin to crystallize spinel above 1500°C and reach

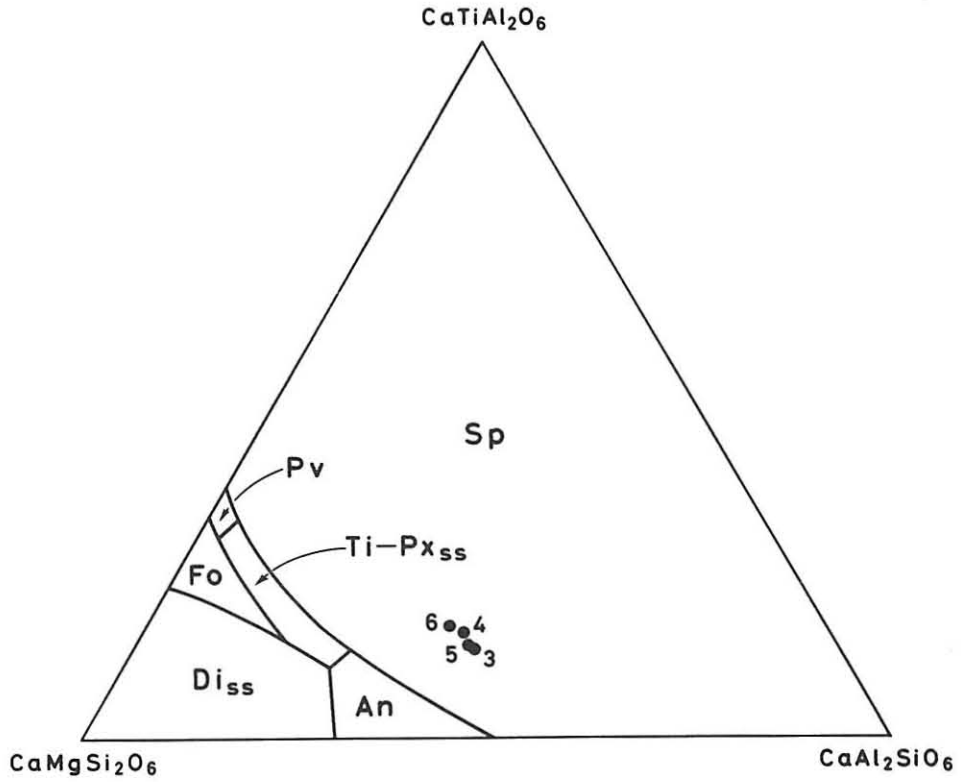

Fig. 7 Projection of Type B inclusions in the Allende meteorite on the Di-CaTs-Tp basal join form Sp(spinel) apex.

the spinel field of the join Di-CaTs-Tp at about 1400°C. At 1300°C the second phase anorthite begins to precipitate and within a temperature range of 70°C crystallization of other phases begin and solidus is attained. Di(40)CaTs(40)Tp(20) crystallizes to an assemblage of spinel + anorthite + perovskite + melilite + Ti-pyroxene(ss), whereas Di(50)CaTs(40)Tp(10) ceases the crystallization on an univariant line and perovskite is absent in the final assemblage (spinel + melilite + anorthite + Ti-rich diopside(ss)). Therefore, the slight difference of the starting composition causes the different final assemblage with or without perovskite. This would explain the observation that perovskite is absent in some inclusions.

According to Grossman (1975) the crystallization sequence of Type B inclusions is anorthite, Ti-pyroxene, melilite. Blander and Fuchs (1975) reported eutectic intergrowth and Kurat et al. (1975) considered that melilite and Ti-pyroxene crystallize at almost the same time followed by anorthite. Judging from texture and the mineral paragenesis, however, the minerals in question would be crystallized within a small temperature range as in the case

of the compositions of Type B inclusions in the join Di-CaTs-Tp and the small difference in composition in a multi-component system probably gives the different order of crystallization, but this is not so serious a problem to the mechanism of the formation of the inclusion. The significance is that spinel is a first phase in crystallization and has a long crystallization range. Finally it is followed by anorthite, melilite, Ti-pyroxene with or without perovskite within a small temperature range near the solidus as shown in the present study.

Formation of Type B Inclusion

It is clear from the texture that the inclusions passed a liquid state. Blander and Fuchs (1975) suggested that the inclusions crystallized from "metastable subcooled liquid droplets" which are directly condensed from the nebula. On the contrary, Grossman and Clark (1973) and Grossman (1975) considered aggregates consisting of spinel, anorthite, melilite, perovskite, and clinopyroxene were formed by condensation from vapor and then melted by lightning discharge or the impact between the aggregates as proposed by Whipple (1966, 1972) and Cameron (1966, 1973). Grossman and Gnapathy (1976) suggested that the Ti-pyroxene is crystallized from the liquid formed by melting of condensed materials. Clayton et al. (1977) proposed the following

Table 5 Calculated compositions of Type A inclusions (Grossman, 1975) and Norms

Chemical composition		
	i	ii
CaO	29.71	36.49
Al_2O_3	41.75	35.07
TiO_2	0.84	0.79
MgO	9.72	5.43
SiO_2	17.99	22.20
Total	100.01	99.98
	Norm	
Pv	1.5	1.4
Geh	60.0	74.3
Ak	11.2	13.6
Sp	27.2	10.4
Total	99.9	99.7
Comp. of melilite	Ak16	Ak15

Pv=$CaTiO_3$, Geh=$Ca_2Al_2SiO_7$, Ak=$Ca_2MgSi_2O_7$, Sp=$MgAl_2O_4$

mechanism: All the solid phases were condensed from vapor, and then reacted with vapor to form liquid with cooling. Finally the assemblage spinel + liquid is obtained at about 1520°K (1350°C), and from this liquid clinopyroxene, anorthite, and melilite crystallize below 1500°K (1230°C) at 10^{-2} atm. In the present study, the temperature of an invariant point at which clinopyroxene, anorthite, melilite, and perovskite coexist is 1500°K (1230°C) which agrees with the temperature estimated by Clayton et al. (1977). The melting of aggregates of spinel + anorthite + melilite + clinopyroxene + perovskite occurs at 1570°K to leave the assemblage spinel + liquid. The temperatures of the beginning of spinel + liquid assemblage and of the crystallization of the other phases are little higher than that estimated by Clayton et al. (1977). This is probably caused by the difference of pressure. The projections of Type B inclusions show that the melting aggregates in different compositions at this temperature always gives the liquid the same composition. This phenomena are also observed in Type A inclusions as shown in Table 5. When the compositions are calculated in terms of Ak($Ca_2MgSi_2O_7$), Geh($Ca_2Al_2SiO_7$) and Sp, the rations Ak:Geh:Pv are similar to each other.

These facts suggest that spinel is formed in different ways from the other minerals as suggested by some authors (cf. Clayton et al. 1977).

Acknowledgement

This paper is dedicated to Prof. Kenzo Yagi on the occasion of his retirement from the chair. He inspired K.O. to study experimental petrology and M.K. to study meteorite. We wish to express our sincere gratitude for his encouragement and advice during the study. Thanks are also due to the following persons: Dr. N. Stevens of Queensland University for his critial reading of the paper in manuscript, Mr. H. Kuwahata of the Faculty of Engineering, Hokkaido University for his help in E.P.M.A. analyses, Mr. S. Terada and Mrs. S. Yokoyama of Hokkaido University for their help in drawing figures and typing manuscript. Part of the cost for the present study was defrayed by the Grant for Scientific Research from the Ministry of Japan, No. 25468.

References

Blander, M. and Fuchs, L.H., 1975. Calcium-aluminium-rich inclusions in the Allende meteorite: Evidence for a liquid origin. *Geochim. Cosmochim. Acta,* 39: 1605-1619.

Cameron, A.G.W., 1966. The accumlation of chondritic material. *Earth Planet. Sci. Lett.,* 1: 93-96.

Cameron, A.G.W., 1973. Accumlation processes in the primitive solar nebula. *Icarus,* 18: 407-450.

Clark, S.P., Schairer, J.F., and DeNeufville, J., 1962. Phase relations in the system $CaMgSi_2O_6$-$CaAl_2SiO_6$-SiO_2 at low and high pressure. *Carnegie Inst. Wash. Year Book,* 61: 59-68.

Clayton, R.N., Onuma, N., Grossman, L., and Mayeda, T.K., 1977. Distribution of the pre-solar component in Allende and other cabonaceous chondrites. *Earth Planet. Sci. Lett.,* 26: 140-144.

Grossman, L., 1975. Petrography and mineral chemistry of Ca-rich inclusions in the Allende meterorite. *Geochim. Cosmochim. Acta,* 39: 433-454.

Grossman, L. and Clark, S.P., Jr., 1973. High-temperature condensates in chondrites and the environment in which they formed. *Geochim. Cosmochim. Acta,* 37: 635-649.

Grossman, L. and Ganapathy, R., 1976. Trace elements in the Allende meteorite-I. Coarse-grained, Ca-rich inclusions. *Grochim. Cosmochim. Acta,* 40: 331-344.

Marvin, V.B., Wood, J.A., and Dickey, J.S., Jr., 1970. Ca-Al-rich phases in the Allende meterorite. *Earth Planet. Sci. Lett.,* 7: 346-350.

Mason, B., 1974. Aluminum-Titanium-rich pyroxenes, with special reference to the Allende meteorite. *Am. Mineral.,* 59: 1198-1202.

Onuma, K., Hijikata, K., and Yagi, K., 1968. Unit-cell dimensions of synthetic titan-bearing clinopyroxenes. *Jour. Fac. Sci., Hokkaido Univ., Ser. IV,* 14: 111-121.

Onuma, K. and Yagi, K., 1971. The join $CaMgSi_2O_6$-$Ca_2MgSi_2O_7$-$CaTiAl_2O_6$ in the system CaO-MgO-Al_2O_3-TiO_2-SiO_2 and its bearing on titanpyroxenes. *Mineral. Mag.,* 38: 471-480.

Onuma, K. and Yagi, K., 1975. The join $CaMgSi_2O_6$-$CaAl_2SiO_6$-$CaFe^{3+}AlSiO_6$ in air and its bearing on fassaitic pyroxene. *Jour. Fac. Sci., Hokkaido Univ., Ser IV,* 16: 343-356.

Whipple, F.L., 1966. Chondrules: suggestions concerning their origin. *Science,* 153: 54-56.

Whipple, F.L., 1972. On certain aerodynamic processes for asteroids and comets. in *From Plasma to Planet,* Ed. A. Elvius, Almqvist and Wicksell.

Yagi, K. and Onuma, K., 1967. The join $CaMgSi_2O_6$-$CaTiAl_2O_6$ and its bearing on the titanaugites. *Jour. Fac. Sci., Hokkaido Univ., Ser IV,* 13: 463-483.

Yagi, K. and Onuma, K., 1969. An experimental study on the role of titanium in alkalic basalts in light of the system diopside-akermanite-nepheline-$CaTiAl_2O_6$. *Am. Jour. Sci., Schairer Vol.,* 267-A: 509-549.

Yang, H.Y., 1973. Synthesis of an Al-and Ti-rich clinopyroxene in the system $CaMgSi_2O_6$-$CaAl_2SiO_6$-$CaTiAl_2O_6$. *EOS,* 54: 478.

(Received on Oct. 27, 1977)

Appendix

After the present work had been completed, we noticed that the paper "The join $CaMgSi_2O_6$-$CaAl_2SiO_6$-$CaTiAl_2O_6$ and its bearings on the origin of the Ca- and Al-rich inclusions in the meterorites" was published by H.Y. Yang in Proceed. Geol. Soci. China, No. 19, 107-126, 1976. The liquidus diagram presented by this author is in good agreement with the present study. He also confirmed the invariant assemblage Ti-pyroxene + anorthite + spinel + perovskite + melilite + liquid at 1222°C, which is slightly lower than that obtained in the present study, 1230° ± 5°C. Yang reported that melilite is almost always present at subsolidus temperatures below 1230°C. On the other hand, in the present study melilite crystallizes even at 1300°C from the compositions in the Di-poor region.